



Feasibility study of oil-on-water cooling in high-speed end milling of hardened steel

Shixiong Wu¹ · Jundong Bi¹ · Zhiyang Li¹ · Hongchang Liao¹ · Chengyong Wang¹ · Lijuan Zheng¹

Received: 23 April 2019 / Accepted: 28 January 2020 / Published online: 14 February 2020
© Springer-Verlag London Ltd., part of Springer Nature 2020

Abstract

The machining efficiency of hardened steel molds can be significantly improved through high-speed deep milling. However, under these circumstances, the temperature and milling force increase greatly, and the end mills are subjected to rapid wear. A feasibility study of the oil-on-water (OoW) method in the high-speed end milling of P20 hardened steel was conducted. The experimental results show that the tool life of OoW is significantly longer compared with that of dry cutting and compressed air cooling. Moreover, the OoW method promotes tool life under low- and high-speed milling conditions. Thermal wear phenomena (e.g., adhesion) are evidently suppressed, and the development of the milling force and tool wear is considerably slowed down in OoW processing. The main reason for the excellent cooling and lubrication performance of the OoW method is that a two-layer film (oil film + water film) is formed when the OoW droplets collide with the cutting interface. The evaporation of the water film removes much heat and prevents the high-temperature failure of the oil film. Moreover, the single use of oil mist and water mist leads only to a single-layer film, resulting in an evidently shorter tool life than that of the OoW method. In the OoW cutting process, the chipping belt of the flank face is discontinuous, and the wear of the adhesion/attrition is less severe compared with those of the other processing modes. In addition, the tool wear and chipping belt occur with a certain amount of material peeling, and the thermal fatigue and mechanical behavior of the tool substrate in a certain temperature range are the main reasons for the discontinuity of the chipping belt in the OoW process.

Keywords Hardened steel · High-speed milling · Oil-on-water · Tool wear

Nomenclature

a_p	Axial depth of cut
a_e	Radial depth of cut
α	Spraying angle
V_c	Cutting speed
f_z	Feed per tooth
R_a	Surface roughness
F_x	Force in the x -direction
F_y	Force in the y -direction
T_o	Object surface temperature
T_j	Coolant jet temperature
k	Heat transfer coefficient
S	Spalling width of materials

D_f	Depth of chipping on flank face
D_r	Depth of chipping on rake face

1 Introduction

Hardened steel is a difficult-to-machine material with hardness values ranging from 45 to 65 HRC. This material has been widely used to manufacture molds owing to its good wear resistance and high hardness. These hardened molds are frequently processed with carbide spiral end mills. To exploit the side milling capability of the end mill and improve its cutting efficiency, a deep axial depth of cut (a_p) and a short radial depth of cut (e.g., $a_e \leq 1.0$ mm) are often chosen in the actual machining process [1]. The machining efficiency can be remarkably improved by significantly increasing the axial depth of cut a_p of the end mill. This machining approach for spiral end mills is known as “deep milling” [2]. Moreover, the material removal rate can be significantly improved through the high-speed deep milling mode. However, the temperature

✉ Shixiong Wu
151688386@qq.com

¹ Mechanical and Electrical Engineering Institute, Guangdong University of Technology, Panyu Higher Education Mega Center, Guangzhou 510006, China

and milling force increase significantly with the milling of hardened steel, which may lead to a rapid tool wear. Therefore, investigating tool wear of different cooling methods in the high-speed deep milling process of hardened steel is important for mitigating tool loss and improving the deep cutting capacity and machining efficiency.

Flood cooling has been widely used during turning and milling to minimize the high temperature of the tool's cutting edge. However, it pollutes the environment and affects the health of workers. Moreover, this method results in high production costs. Dry cutting with a coated tool is the ideal method for hardened steel processing because it causes no contamination and does not require additional auxiliary devices or equipment during processing. Although the coating technology has developed significantly, the rapid wear of coated cutting tools remains a problem in the processing of difficult-to-machine materials such as hardened steel. Compressed air cooling is a pollution-free cooling method that is commonly used in deep milling. Compared with dry cutting, compressed air cooling can transfer the heat of the cutting area more effectively, thereby reducing the cutting temperature and prolonging the tool life. However, because the heat transfer coefficient of compressed air cooling is not sufficiently high, the improvement of the tool life is limited. A better cooling method must be determined through further research.

Some reinforced cooling methods, e.g., carbon dioxide cooling, LN cooling, and cryogenic air cooling, are applied to difficult-to-cut materials, as they can effectively lower the temperature of the tool and workpiece, improve the cutting surface quality, and reduce the tool wear. According to the high-speed cryogenic finish machining experiment of titanium alloy Ti-6Al-4V by Schoop et al. [3], tool wear under conventional flood cooling is more than 4–5 times higher compared to the cryogenic conditions. Sun et al. [4] found that applying cryogenic compressed air significantly increased the tool life compared with dry machining. Further, the increase in tool life is more significant at higher cutting speeds, as the plastic deformation of the cutting edge occurring during dry machining was suppressed by the cryogenic compressed air cooling. Stephenson et al. [5] performed a rough turning on the Inconel 750 alloy with supercritical CO₂. The results indicate that supercritical CO₂ increases the tool life or the material removal rate, compared to aqueous flood coolants, by improving the lubricity and changing the dominant wear mechanism from rapid notch wear to gradual crater wear and chip hammering. Nevertheless, the three reinforced cooling methods are costly both in usage and equipment. Considering the expenditures, these forced cooling methods are less recommended for adoption in the high-speed milling of hardened steels.

Minimum quantity lubrication (MQL) is a green cooling method developed on the basis of compressed gas. The mixed atomization of compressed gas and micro-oil was sprayed to

the cutting zone to exert a good lubrication effect. To avoid oil fog pollution, the oil flow rate is controlled to lower than 50 mL/h. Liao et al. [6] studied hardened steel high-speed milling by applying the MQL method and found that using MQL can delay the welding of chips onto the tool and, hence, prolong the tool life when compared with dry cutting. Khettabi et al. [7] investigated the performance of MQL and the dry high-speed milling of aluminum alloys. Their results indicated that the increase in the flow rate lubrication of the MQL system decreased the cutting force and increased the particle emission during the milling process. Ganguli and Kapoor [8] investigated the effectiveness of an atomization-based MQL spray system. The low-speed end-milling experimental results showed that the MQL approach exhibited a lower cutting force and a higher surface finish, and the tool life was extended up to 75% over flood cooling.

MQL has good lubricating performance, but its cooling effect is insufficient. In some high cutting heat processing situations, MQL has the problem of high-temperature failure of lubricating oil. To solve this, a new method known as oil-on-water (OoW) has been proposed. OoW uses MQL for lubrication and the phase transformation of water droplets for the improvement of cooling performance. The OoW microdroplet gas jet is formed by mixed atomization of micro-oil and a small amount of water with compressed gas. Yoshimura et al. [9] developed an OoW nozzle system. Its application to the grooving process in the production line of engine primary bearings showed that the developed system can improve the tool life. In an experimental study of turning an aluminum silicon alloy, Itoigawa et al. [10] found that OoW yielded good lubrication performance if the appropriate lubricant, e.g., synthetic ester, was used. According to the OoW turning experiments for compacted graphite cast iron by Wang et al. [11], a lower adhesion on both the tool rake and the flank faces and a lower tool wear rate were obtained because of the OoW's combined effects of cooling and lubrication. OoW is a promising green cooling method. However, there is little literature on the research of milling under OoW condition so far. This paper intends to apply OoW to high-speed deep milling of hardened steel. The corresponding machining effect and tool wear mechanism need to be studied.

The interaction between the chip, tool, and workpiece in the cutting process usually causes tool wear and breakage. The wear/breakage mechanisms include abrasion, adhesion, attrition, diffusion, thermal fatigue, mechanical shocks, and chipping. Abrasion wear occurs when hard particles of the workpiece and particles removed from the tool rub against the tool flank or rake face. According to Junior et al. [12], abrasion is the main mechanism in the beginning stage of tool life, and the abrasion wear land generally displays scratches parallel to the

cutting direction. In addition, adhesion is the welding of the workpiece material onto the rake or flank face of the tool; it occurs after the coating has worn out. Attrition is closely connected to adhesion; it can be defined as the cyclical adhesion and removal of chip/workpiece material from the tool. During the process, some tool particles are torn out, and rough tool surfaces are formed. Furthermore, diffusion wear during cutting includes the transfer of atoms between the chip/workpiece and tool; high temperatures have an important influence on diffusion wear. According to Nouari and Ginting [13], the diffusion of cobalt and carbon is typical when a carbide tool is used for cutting; it may reduce the roughness and increase the brittleness of the tool. During milling, the tool experiences a great thermal shock and mechanical impacts in each revolution, and cracks, chipping, and fractures are likely to occur [14]. For hardened steel milling, most studies of tool wear and damage mechanisms of coated carbide tools have been conducted on dry cutting; however, few have investigated MQL. Dolinšek et al. [15] performed hardened steel high-speed milling experiments and discovered that abrasion, oxidation, and adhesion wear are the major causes of coated tool wear. Moreover, Wang et al. [16] used two types of coated carbide tools to study the tool wear mechanism in the high-speed milling process of hardened steel. Their experimental results indicate that the dominant wear patterns include rake and flank wear, breakage, and microchipping. In the MQL-employed finish hard milling process with ball-nose end carbide cutters in [17], the major tool damage mechanisms were notch wear, adhesion, and chipping. Moreover, in an MQL cutting study, Liao et al. [6] observed adhesion and groove wear during the high-speed end milling of NAK80 hardened steel. When the oil-on-water (OoW) cooling method is used in the high-speed deep milling process of hardened steel, the tool wear evolution and evolution mechanism may be different from the ones previously mentioned.

In this study, the OoW method in a high-speed deep milling process was studied. The cooling effect, tool wear process, and tool wear mechanism of the OoW process are discussed with the commonly used dry cutting and compressed air cooling methods. To the best of the authors' knowledge, no similar research study has been conducted. The remainder of this paper proceeds as follows. Section 2 introduces the three cooling approaches and experimental processes; Sections 3 and 4 discuss the experiment results, and Section 5 provides the conclusion.

2 Experimental procedure

The machined material P20 mold steel (Table 1) is suitable for large- and medium-sized precise molds with good hardness and machinability. The material hardness can reach 50–54 HRC after quenching, and the dimensions of the hardened steel P20 workpiece are 25 mm × 90 mm × 300 mm.

Carbide four-flute spiral end mills (Table 2) manufactured by Zhuzhou Cemented Carbide Cutting Tools Co., Ltd. were selected to compare the cutting performances in different cooling processes. The radial and axial rake angles of the tool are 10° and 45°, respectively, and the elements in the tool coating are Ti, Al, Si, and N. The microstructure of the carbide substrate of the end mill is shown in Fig. 1a. The carbide grains are very fine, and the sizes of most grains are below 0.8 μm. Moreover, the substrate of the cemented carbide tool comprises mainly a WC hard phase, Co bonded phase, and small amounts of Ti, Cr, and Nd carbides (TiC, CrC, and NdC). These small carbide amounts improve the hardness, strength, and wear resistance of the cemented carbide matrix.

The schematics of the different cooling mechanisms are shown in Table 3. The OoW method and compressed air cooling method share the same equipment, and the pressures and flow rates of the compressed air are equal. In the compressed air cooling method, the compressed air is directly sprayed with an air gun. In the OoW cutting method, micro-oil and small amounts of water and compressed air are transported to an air gun and subsequently atomized, mixed, and sprayed onto the tool. The key spraying conditions (e.g., spraying angles) and oil–water proportion are crucial for the cooling and lubrication performance. The lubricant oil used in the OoW cooling method is synthetic ester (2000-35) with a viscosity (40 °C) of 30 and flash point of 300 °C.

The high-speed deep milling test was performed on the MILLTAP 700 machining center (Fig. 2). After each milling process was completed, the flank wear of the cutting tool was measured with a twin optics video system (MARCEL AUBERT). To learn the microcosmic conditions of tool wear and breakage, scanning electron microscopy (NanoSEM430) was used for further meticulous observation. The chip morphology was observed by a micro three-dimensional (3D) scanner (Alicona). The cutting force was measured using a three-axis dynamometer (Kistler9257B) and a multichannel charge amplifier.

The primary cutting parameters are the hardened steel milling parameters recommended by the factory (Table 4),

Table 1 Major chemical compositions and hardness of P20 steel

Workpiece material	C	Mn	Cr	Mo	Si	P, S	Hardness
P20	0.28–0.4	0.6–1	1.4–2	0.3–0.55	0.2–0.8	< 0.03	HRC 50–54

Table 2 Parameters of end mill

Tool coating	Tool matrix material	Diameter	Radial rake angle	Axial rake angle	Clearance angle	Helical angle	Number of teeth	Model
Ti, Al, Si, N	C, W, Co	φ 8 mm	10°	45°	2°	45°	4	HMX-4E-D8.0

and the axial depth of cut was increased from 4 to 8 mm. In actual high-speed milling processes, speeds in the range of 100–200 m/min are more common. Based on this, the machining experiments at this cutting speed range were conducted with the same material removal amount per tooth ($f_z a_p a_c$). Machining was conducted through the dry cutting, compressed air cooling, and OoW methods based on two sets of cutting parameters. To improve the accuracy of the tool rotation and ensure the balanced wear of the four cutting edges of the end mill, a precise shrink-fit holder was employed. Moreover, climb milling was selected for the experiments.

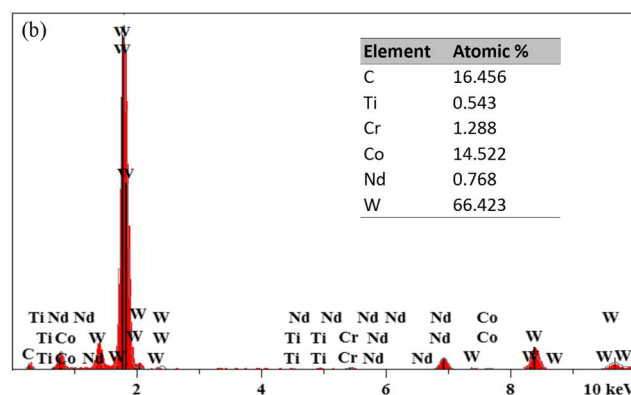
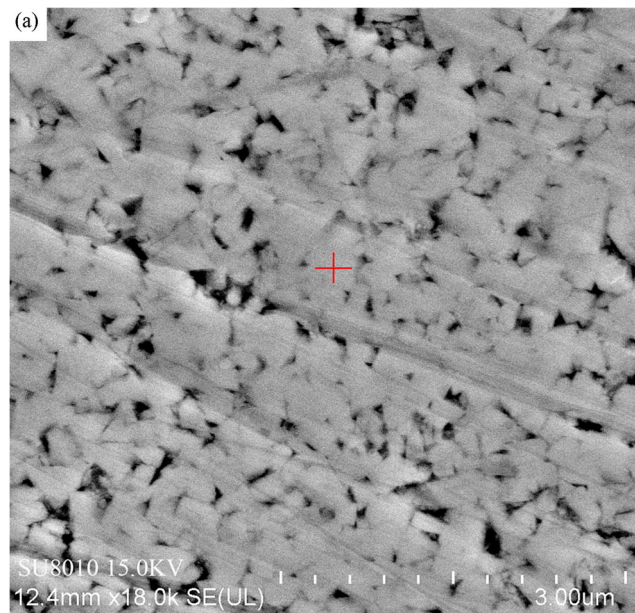


Fig. 1 Analysis of tool substrate of spiral end mill. **a** Microstructure. **b** X-ray energy-dispersive spectroscopy (EDS) results

3 Experimental results and discussion

3.1 Determining the optimal spraying conditions for OoW milling

On the experimental conditions, the oil flow rate was set as 20 mL/h. Larger values may bring a risk of air pollution. In addition, a normal flow rate (90 L/min) was chosen for the compressed air, similar to that in [9]. If the flow rate of the compressed air is increased, the energy consumption increases. Because the spraying angle and water flow rate are important parameters, two related experiments were conducted to optimize the two parameters.

3.1.1 Spraying angle

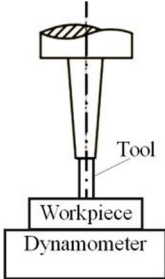
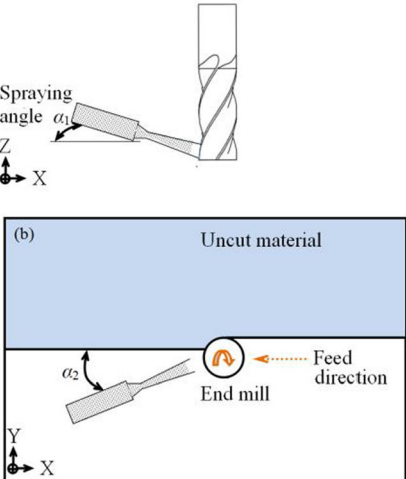

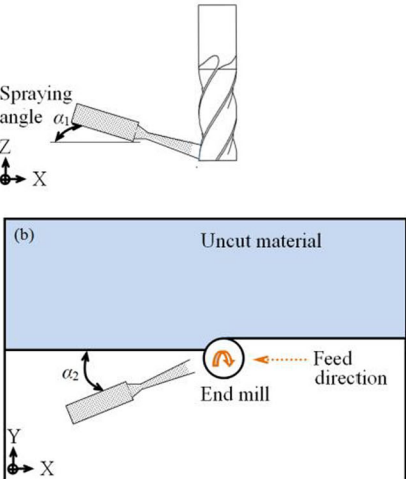
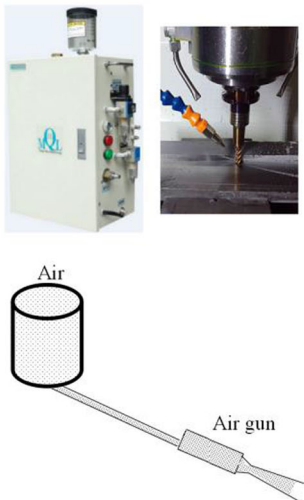
Figure 2 shows the spraying angle diagram. The vertical spraying angle (α_1) was set to 45° to spray the rake and flank faces. Different horizontal spraying angles (α_2) have different effects during processing. Figure 2b illustrates four different horizontal spraying angles. When the axial depth of cut is short, the gas jet can easily reach and cover the cutting zone of the tools. However, with a long axial depth of cut (deep milling), the gas emitted at angles 2 or 4 is blocked by the surface of the workpiece and can hardly reach the tool bottom. Thus, horizontal spraying angles 1 and 3 were chosen for the experiment.

A comparative experiment was conducted between angles 1 and 3, and the results are shown in Fig. 3. Compared with angle 3, angle 1 can delay the process of tool wear and improve the tool life by 34%. The experimental results of López de Lacalle et al. [18] also proved faster tool wear at angle 3. The reason may lie in two factors. First, the direction of the air jet in the horizontal spraying angle 3 is against the chip-flow direction. The chip flow is impeded by the jet, which will introduce more heat from the chips to the tool. Second, when blocked by chips, the air jet cannot enter the cutting contact zone to effectively cool and lubricate it. Consequently, the tools in spraying angles 3 wear out more quickly than in spraying angles 1.

3.1.2 Flow rate of water

The oil–water ratio is an important technological factor in the OoW cooling method. At a constant oil flow rate, a

Table 3 Cooling conditions

Cooling approach	Conditions	Diagrammatic sketch	Equipment
Dry cutting	Natural cooling in air		none
OoW	Oil: 20 mL/h; Water: 50 mL/h, 200 mL/h, 500 mL/h; 1000 mL/h; 2000 mL/h. Air pressure: 0.5 MPa; Air: 90 L/min; Temperature: 25 °C; Spraying angle approach: $\alpha_1=45^\circ$, $\alpha_2=30^\circ$.		
Compressed air cooling	Air pressure: 0.5 MPa; Air: 90 L/min; Temperature: 25 °C; Spraying angle approach: $\alpha_1=45^\circ$, $\alpha_2=30^\circ$.		

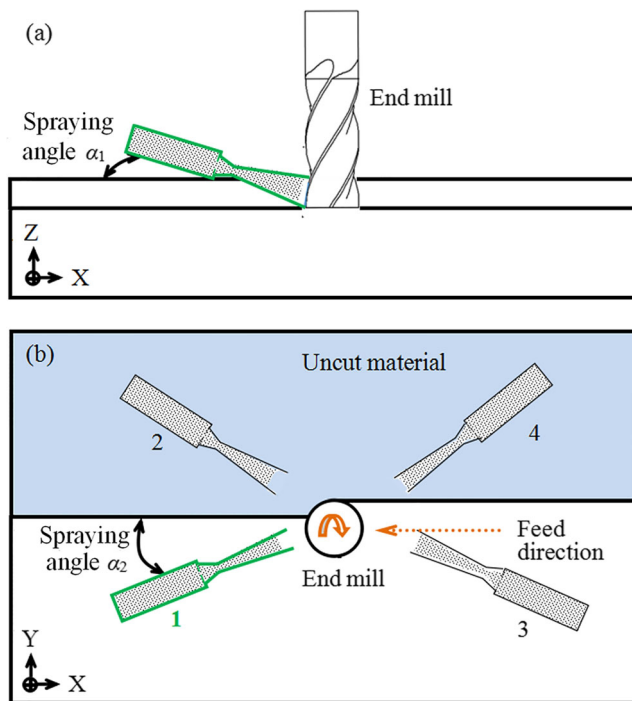


Fig. 2 Spraying angles. **a** Spraying angle α_1 in vertical plane. **b** Spraying angle α_2 in horizontal plane

proper water flow rate results in better lubrication and cooling functions. Five water flow rates (50, 200, 500, 1000, and 2000 mL/h) were adopted in the OoW milling experiments. The corresponding results are shown in Fig. 4. The tool life at 200 mL/h is the longest. Only when the water flow rate is set appropriately (200 mL/h in this study), massive tiny OoW droplets, which can easily enter and cool the cutting zone (Fig. 4b), can be formed and distributed. Under this condition, the droplets present the OoW state and yield a good lubricating effect. When the water flow rate is very small (50 mL/h), the oil–water ratio approaches 0.4. In this state and at high temperatures, the atomized OoW droplets tend to boil and sputter. Therefore, the cooling and lubrication effects are negatively affected. Furthermore, when the water flow rate is high (e.g., 1000 and 2000 mL/h), the atomized water droplets encapsulate the oil (Fig. 4b), which weakens the lubricating effect. Under this condition, the droplets are large and cannot be evenly dispersed on the tool surface; this may result in a higher local thermal stress. In addition, tools with high water flow rates (1000 and 2000 mL/h) experience more and stronger discontinuous chipping compared

Table 4 Cutting parameters

V_c (m/min)	f_z (mm/z)	a_p (mm)	a_c (mm)	$f_z a_p a_c$
170	0.0269	8	0.5	1.077
130	0.0337	8	0.4	1.077

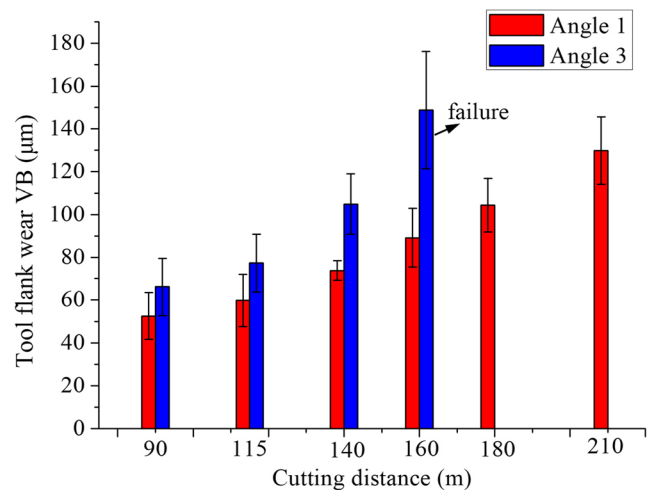


Fig. 3 Comparison of tool wear of spraying angles 1 and 3 ($V_c = 170$ m/min, $f_z = 0.0269$ mm/z, $a_p = 8$ mm, $a_c = 0.5$ mm, water 200 mL/h, oil 20 mL/h)

with those at 200 mL/h. This phenomenon may be related to the uneven thermal change and heat stress. When the water flow rate is increased, the injection state approaches the cutting fluid processing conditions. According to [6, 19], large temperature gradients and thermal stresses are easily generated under the cutting fluid processing conditions. However, according to the scanning electron microscopy (SEM) results of this study, tools treated with 1000 and 2000 mL/h do not exhibit thermal cracks perpendicular to the cutting edge, such as in [6, 19]; moreover, only several mechanical cracks parallel to the cutting edge were observed (Fig. 4c). The result may be related to the tool material characteristics (Fig. 1). The thermal stress is below the strength of the tool material and does not cause thermal cracking. In the following section, the relationship between chipping, thermal stress, and the tool material will be further discussed.

3.2 Cutting at a low speed (130 m/min)

3.2.1 Tool wear process

Figure 5 shows the tool flank wear with respect to the accumulative cutting distance for the three machining approaches. The wear curve of the dry cutting method is very steep. The initial, stable, and fast wear stages cannot be clearly distinguished because tool wear exacerbates very fast in the dry cutting process. The tool of the compressed air cooling approach reaches a short steady wear stage between the cutting distances 65 and 90 m after the initial rapid wear; subsequently, the flank wear of the tool increases dramatically, and catastrophic chipping occurs. The tool of the OoW approach experiences a longer steady wear stage at a cutting distance of 65–115 m; afterward,

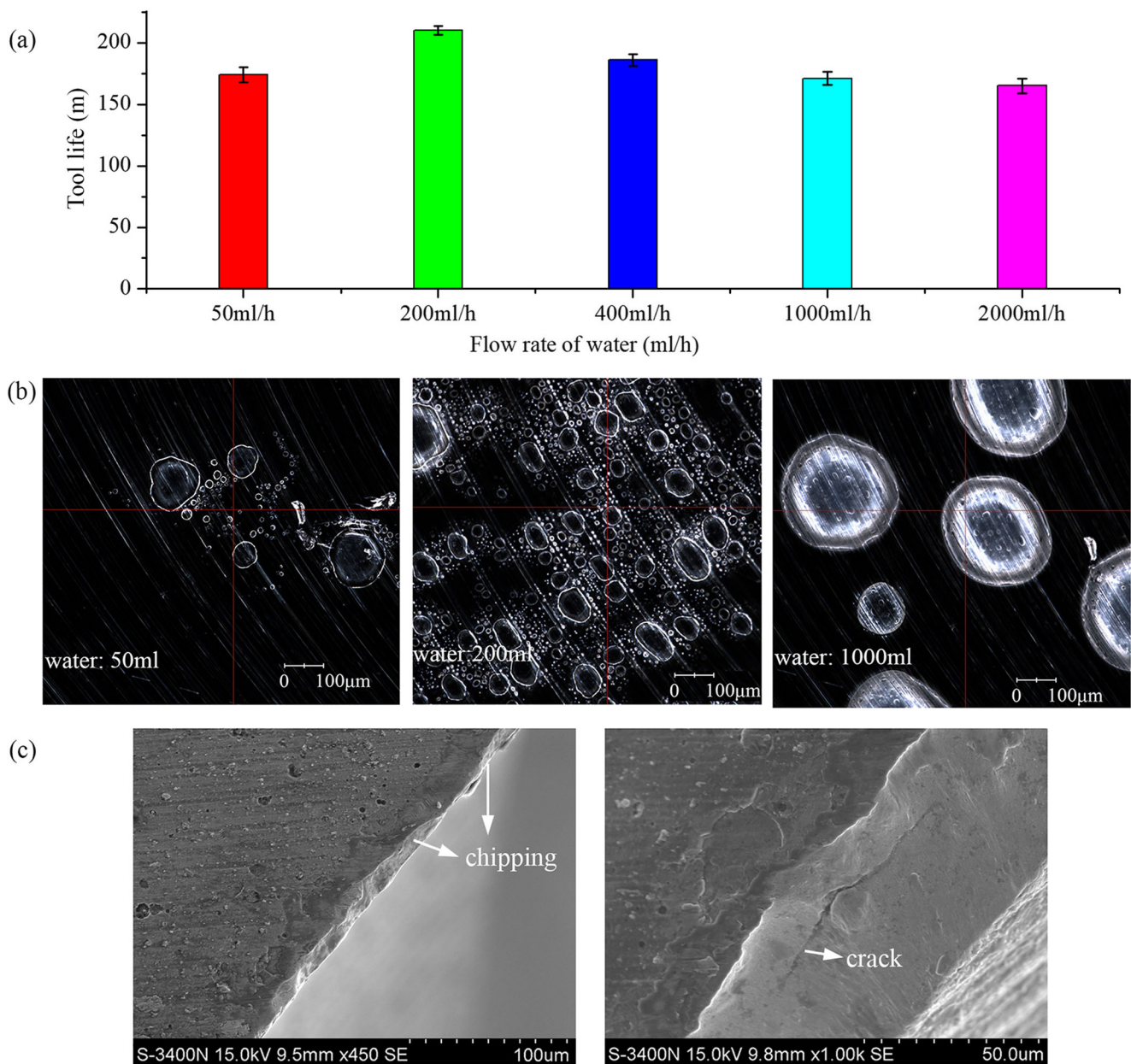


Fig. 4 Comparison of tool wear at different water flow rates and cutting distance of 135 m ($V_c = 170$ m/min, $f_z = 0.0269$ mm/z, $a_p = 8$ mm, $a_c = 0.5$ mm, oil 20 ml/h): **a** comparison of tool life; **b** OoW droplets at 50,

200, and 1000 mL/h; **c** discontinuous chipping of tool and cracks in chipping belt at 2000 mL/h

the tool undergoes a very fast wear stage, in which the curve of the OoW method changes more slowly than those of the other two methods. The maximal flank wear widths VB of the three methods do not exceed the tool wear and failure criteria of $VB = 0.3$ mm, and the main failure form of the tools is catastrophic chipping; $VB = 0.13$ µm is considered the critical value for the tool failure. The tool life was found 90, 133, and 191 m at the cutting speed of 130 m/min for dry cutting, compressed air cooling, and OoW, respectively. Owing to better thermal removal effect, the tool life of compressed air cooling increases by

48% compared with dry cutting. The tool life of OoW is significantly longer than that of the other two methods. Compared with dry cutting and compressed air cooling, the tool life of OoW increases by 112 and 44%. The longer life is closely related to the better heat transfer and lubrication effect of OoW.

3.2.2 SEM analysis of tool wear

Owing to the characteristics of the rake and clearance angles of the spiral end mill (Table 2), the flank face exhibits

OoW: Oil (20 mL/h), Water (200 mL/h), air (0.5 Mpa, 90 L/min).
 $V_c=130$ mm/min, $A_p=8$ mm.

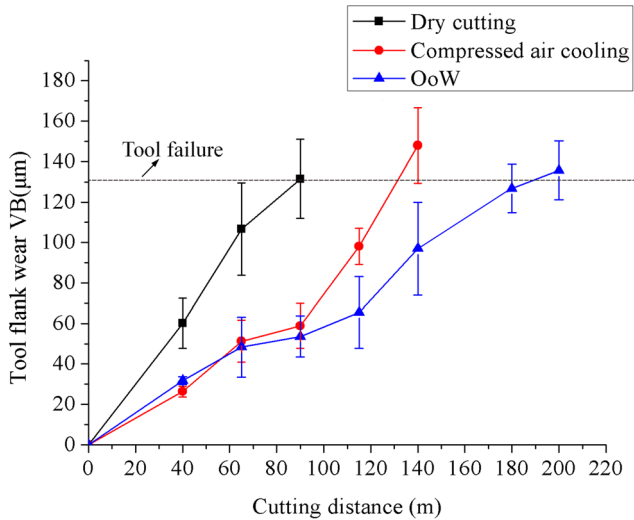


Fig. 5 Tool wear curve of hardened steel deep milling of three methods at 130 m/min cutting speed

more severe wear than the rake face. Figure 6 shows a SEM image of a failed tool used under the dry cutting, compressed air cooling, and OoW methods. The flank can be divided into three areas: zones 1–3. Zones 1 and 2 are the worn areas of the tool, and zone 3 is the area of the flank that remained unchanged. Moreover, zone 1 is the chipping belt, the main part of the flank wear land. The chipping belts of zone 1 of the dry cutting and compressed air cooling methods are relatively continuous, whereas the chipping belt of the OoW approach is relatively discontinuous. The distinct adherent workpiece materials in zone 1 of the dry cutting method experience a higher cutting temperature. Furthermore, there are less adhering workpiece materials in zone 1 in the compressed air cooling and OoW methods than in that of the dry cutting method. In zone 2, ridges and grooves occur parallel to the direction of the cutting speed for all three methods, which is a typical feature of abrasive wear. According to the EDS analysis, the main component of the surface ridges and grooves is tool coating. The dry cutting method leads to much adhering material in zone 2 compared with those of the compressed air cooling and OoW methods. The adhering material is the workpiece material according to the EDS analysis. Zone 3 is the undamaged flank where the tool of the dry cutting method exhibits some bulk bonds; some of the fish scale-like bond widths are greater than 20 µm. By contrast, the compressed air cooling and OoW approaches lead to less adhesion in zone 3, and most bonds have a particle size of below 5 µm. In short, the tool treated with the dry cutting method has more adhered workpiece material in zones 1–3, indicating weaker heat transfer and thermal removal capability and higher cutting

temperatures. The compressed air cooling and OoW approaches result in very light adhesion in zones 1–3 and can control the cutting temperature better. The adhesion degrees of the two methods are similar; however, in the OoW method, the cutting distance is 58 m longer. Therefore, the OoW approach has more effective heat transfer and lubrication properties than the compressed air cooling method.

3.2.3 Evolution of milling force

During the milling process, the sequence of milling force measured by the i time pausing the machining is F_{d-i1} , F_{d-i2} , ..., F_{d-in} ($d=x$ or y), and the effective mean force of the node is calculated by the following formula:

$$F_{d-inms} = \sqrt{\frac{(F_{d-i1}^2 + F_{d-i2}^2 + \dots + F_{d-in}^2)}{n}} \quad (1)$$

The following formula is used to analyze the range of the node force:

$$F_{d-irange} = F_{d-imax} - F_{d-inms} \quad (2)$$

Figure 7 shows the evolution of milling forces under dry cutting, compressed air cooling, and OoW at the cutting speed of 130 m/min. The y -direction force surpasses the x -direction force, indicating that the former is the main cutting force. Figure 7a is the first analyzed. At the beginning of the cut, the milling forces under the three approaches are similar both in the x - and y -directions, so the tools' shear and friction are close to each other before the coating's worn out. The growth rate of cutting force of dry cutting increases the fastest, OoW the slowest, and air cooling is in between. Comparing Fig. 7a and Fig. 5, it can be found that the change trend of milling is consistent with tool wear. Therefore, the enhancing cutting force with increasing cutting length is believed to be due to the evolution of tool wear and tool chipping. Owing to the better thermal removal effect and lubrication ability of OoW than dry cutting and air cooling, tool wear, chipping, and adhesion can be controlled to some extent, which helps delay the evolution process of milling force.

In Fig. 7b, the milling forces under the three approaches show a slow downward trend in the steady and rapid tool wear stages. This may be due to the factor that the tool material of cutting edges gradually peels off as the tool wears.

3.3 Cutting at a high speed (170 m/min)

3.3.1 Tool wear process

Figure 8 shows the tool–flank wear curves under different machining approaches. After the initial rapid wear, the

tool in dry cutting reaches a short steady wear stage at a cutting distance in the range 40–65 m. After that, the flank wear of the tool increases drastically and catastrophic chippings may occur. The tool in compressed air cooling reaches a longer steady wear stage at a cutting distance in the range 50–100 m, and then the tool undergoes very fast wear. The tool in OoW experiences a very long steady wear stage at a cutting distance in the range 40–140 m, and then the accelerating tool wear leads to tool failure. In the fast wear stage, the slope of OoW is smaller than that of the other two methods. Owing to the good cooling and lubricating effects of OoW, the development of tool flank wear is effectively delayed.

When the tools of dry cutting, compressed air cooling, and OoW fail, their flank wear value VB cannot exceed the tool wear criterion of 0.3 mm. The main form of tool failure is catastrophic chipping. When the tool fails, sparks occur in the dry cutting and compressed air cooling cutting. The tool life was estimated as 78, 113, and 210 m at the cutting speed of 170 m/min for dry cutting, compressed air cooling, and OoW, respectively. The tool life of compressed air cooling is increased by 45% compared with dry cutting. The tool life using the OoW method is significantly longer than that for the other two methods. Compared with dry cutting and compressed air cooling, the tool life of OoW is increased by 169 and 86%, respectively. In addition, compared with the properties at a low cutting speed (130 m/min), the tool lives of the dry cutting and compressed air cooling approaches are evidently reduced at a high cutting speed (170 m/min). However, the tool life of the OoW approach is not affected by the cutting speed. Hence, the OoW method has better cooling and lubrication abilities.

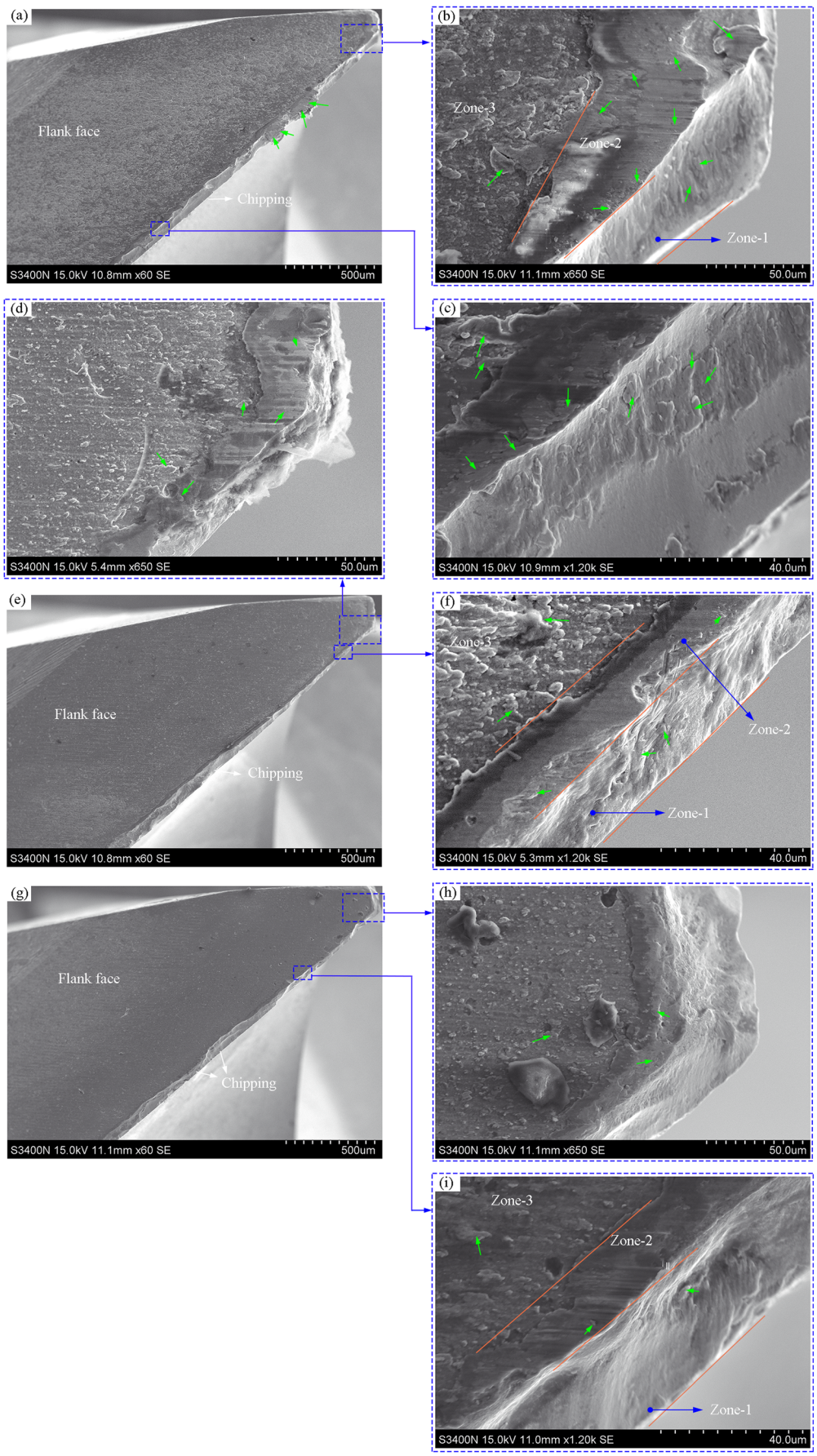
3.3.2 SEM analysis of tool wear

At a high cutting speed, the cutting heat and temperature are often high, and tool wear is more severe. This section describes the tool wear characteristics in more detail.

Figure 9 shows a SEM image of a failed tool for dry cutting. The flank can be divided into three main areas: zone 1, zone 2, and zone 3 (Fig. 9b). Zone 1 is the chipping belt, which is the main part of the flank wear land. In dry cutting, the chipping belt formed on the flank face is relatively continuous (Fig. 9a). This is the area where the blade cuts, squeezes, and rubs. Under high-temperature and high-pressure conditions, the workpiece material is easily welded within the chipping belt. The enlarged views of Fig. 9d and f show that there are some evident adhered materials in the chipping belt of zone 1, which indicates the high cutting temperature. In zone 2, some ridges and grooves parallel to the cutting direction can be seen. This is a typical feature of abrasive wear. The

EDS analysis of the ridges and grooves in Fig. 9c and d shows that the main component is the tool coating element. Moreover, some evident adhered materials can be seen in zone 2, which can be identified as the workpiece material by the EDS analysis. The tip is a special area. By analyzing the tool tip from Fig. 9b, it can be found that a large amount of workpiece material was softened by high temperature and then laterally flowed and bonded to zone 2 and zone 3, indicating a high tip temperature during cutting. Zone 3 is the area of the flank that has not been worn. It is shown in Fig. 9b with large fish scales, each having a width of more than 20 μm . In addition, Fig. 9e and f show the tool from another point of view, with significant adherent workpiece material found on the chipping belts and the flank and rake faces. Moreover, the tool carbide substrate exposed by the adhered material falling off (indicated by the red arrow) can be seen in Fig. 9f. Some tool particles are torn out in this process. In short, the adhesion phenomenon of dry cutting tools is very prominent, indicating the weak thermal diffusion and thermal removal ability as well as the high cutting temperature.

Figure 10 shows a SEM image of a failed tool in compressed air cooling cutting. Similar to dry cutting, compressed air cooling cutting also had very clear zones 1, 2, and 3. The chipping belt of zone 1 shown in Fig. 10a is relatively continuous. In the enlarged view of Fig. 10c and d, there are significant adhered materials (indicated by the green arrow) in the chipping belt of zone 1, which can be known as the workpiece material by EDS analysis. The tool substrate exposed by the adhered material falling off (indicated by the red arrow) can also be clearly seen in Fig. 10c. Some tool particles are torn out in this way. Figure 10c shows the very distinct ridges and grooves in zone 2, whose subject is tool coating according to the EDS analysis. And there is a small amount of adherent workpiece materials in zone 2, lighter than that of dry cutting. In Fig. 10b and d, the workpiece material softened by the high temperature and then laterally flowed and bonded to the surface of the tool can be seen at the tool tip, covering zone 1 and zone 2 and extending to zone 3, but the adhesive degree was not as severe as that of the dry cutting. Zone 3 is the unworn area of the flank face. Zone 3 shown in Fig. 10b and d has some adhered workpiece materials, whose amount is smaller than that of dry cutting, and the size of most bond is less than 10 μm . Overall, the adhesive phenomenon of the cutting 113-m tool in compressed air cooling method is slightly lighter than the cutting 78-m tool in dry cutting, indicating that the former improves the heat transfer to some extent. On the other hand, the compressed air cooling method still showed obvious adhesion during the tool rapid wear stage, which reveals its certain limitations in thermal transfer and thermal removal.



◀ **Fig. 6** SEM images of the worn tool of dry cutting, compressed air cooling, and OoW. **a–c** Dry cutting at the cutting distance of 90 m. **d–f** Compressed air cooling at the cutting distance of 133 m. **g–i** OoW at the cutting distance of 191 m. Green arrows indicate the adhesion materials

Figure 11 shows a SEM image of a tool of OoW at the cutting length of 180 m. Zones 1, 2, and 3 can be clearly identified. The discontinuous chipping belt shown in Fig. 11a is different from that of the previous two methods. From Fig. 11c and d, there is still a small amount of adhesive workpiece materials (shown by green arrows) in the chipping belt of zone 1, as well as the tool substrate (shown by red arrows) exposing after the adhered workpiece material is detached. Overall, the chipping belt had significantly less adhesive than that of the other two methods, which reflects the effective control of the cutting temperature. From zone 2 of Fig. 11c and d, the ridges and grooves caused by abrasive wear and the very small amount of adherent materials are clearly visible. The

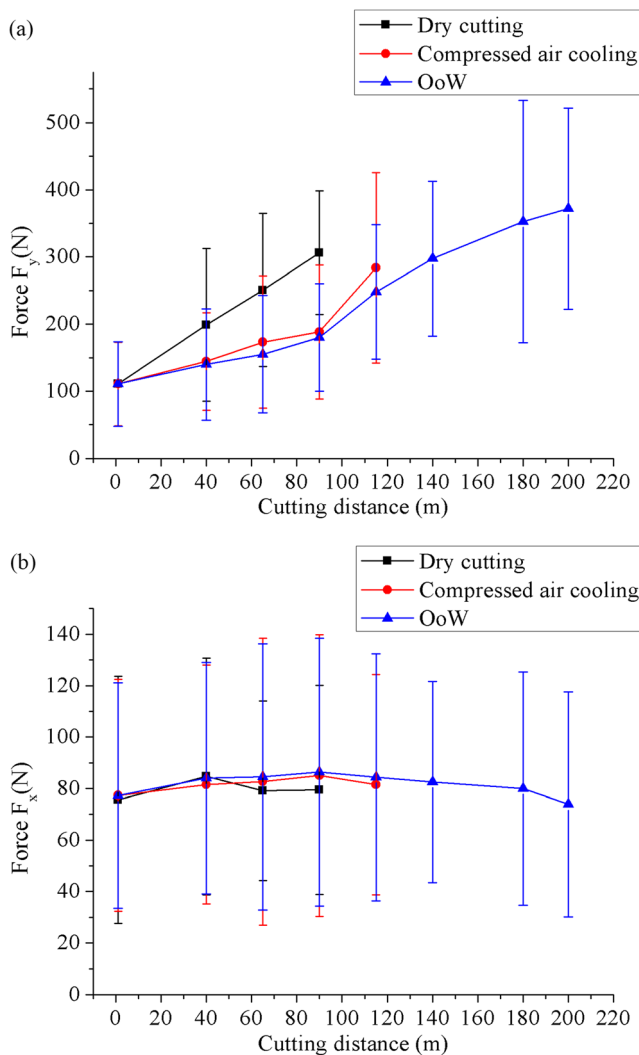


Fig. 7 Milling force at the cutting speed of 130 m/min. **a** y -direction. **b** x -direction

OoW: Oil (20 mL/h), water (200 mL/H), air (0.5 Mpa, 90 L/min). $V_c=170$ mm/min, $A_p=8$ mm.

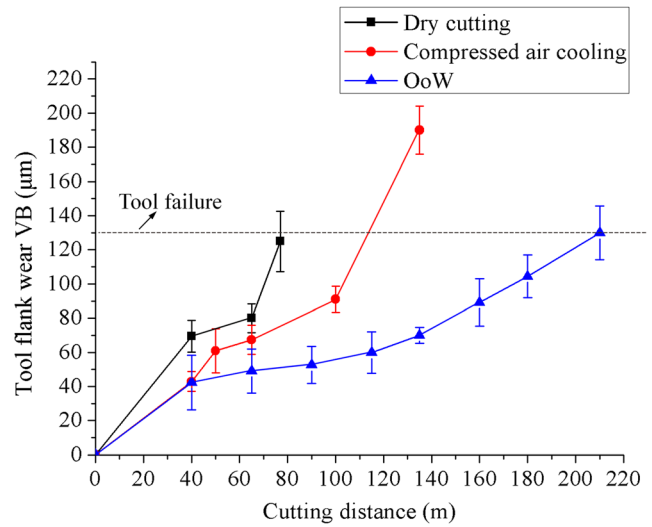


Fig. 8 Tool wear curves of hardened steel deep milling of the three methods at 170 m/min cutting speed

EDS analysis shows that the ridges and grooves are mainly tool coatings, and the adhered material is the workpiece material. Besides, the number and size of the bonded workpiece material in zone 3 (Fig. 11b) is significantly smaller than that of the other two methods. In short, the degree of adhesion from zone 1 to zone 3 of the OoW mode is significantly less than those of dry cutting and air cooling. These phenomena indicate better thermal transfer and thermal removal capabilities of OoW than the other two modes, as well as its effective control of cutting temperature.

3.3.3 Evolution of milling force

Figure 12 shows the evolution of milling forces under dry cutting, compressed air cooling, and OoW conditions. The y -direction force shown in Fig. 12a evidently exceeds the x -direction force in Fig. 12b. So the y -direction force is the main cutting force. This result is consistent with what is shown in Fig. 7.

Figure 12a is analyzed first. At the beginning of the cut, the milling forces of the three approaches are similar both in the x - and y -directions. Thus, the shear and friction of the cutting tools under the three approaches are close to each other before the coating has worn out. When the cutting length exceeded 40 m, evident differences in the milling forces starts to appear, which to some extent reflects that the cooling and lubrication effects of the air jet begins to manifest after the coating has worn out. The milling force of dry cutting increases very rapidly after reaching the cutting length of 40 m, and it exceed 300 N at the cutting length of 70 m. However, the milling force

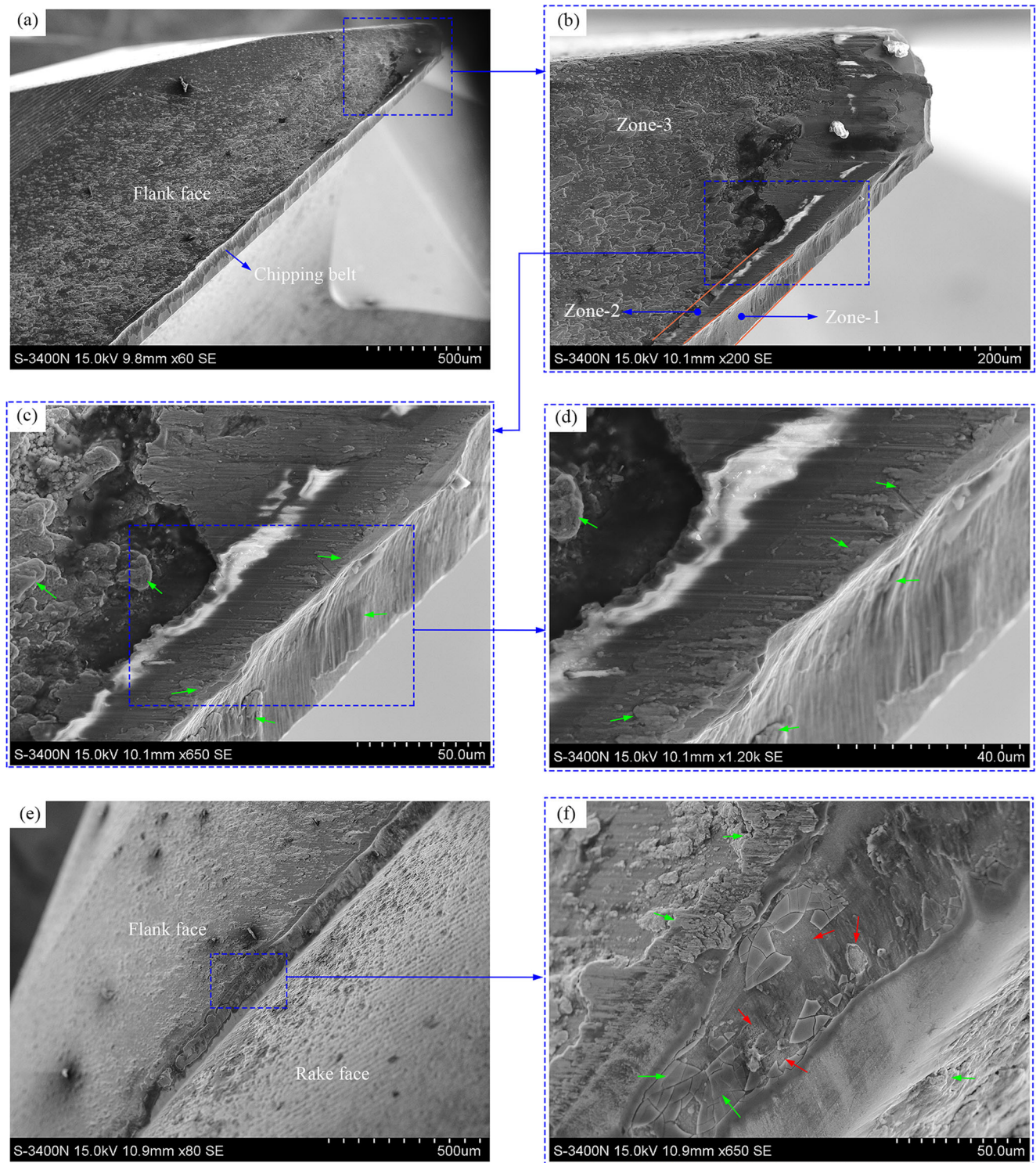


Fig. 9 SEM images of worn tool of the dry cutting method with a cutting distance of 78 m. **a** Flank face of tool. **b** Flank face near the tip. **c** Partial enlarged view. **d** Partial enlarged view. **e** Rake and flank faces and

chipping belt. **f** Partial enlarged view. Green arrows indicate adhering materials, and red arrows indicate detachment of adhering materials

of the OoW mode increases very slowly and exceeds 300 N after the cutting length of 150 m. The milling force variation range of compressed air cooling is between those of dry cutting and OoW. Comparing Fig. 12a and Fig. 8, it

can be found that the change trend of milling is consistent with tool wear. Therefore, the increase in the cutting force with cutting length is believed to result from the evolution of tool wear and tool chipping. Owing to better thermal

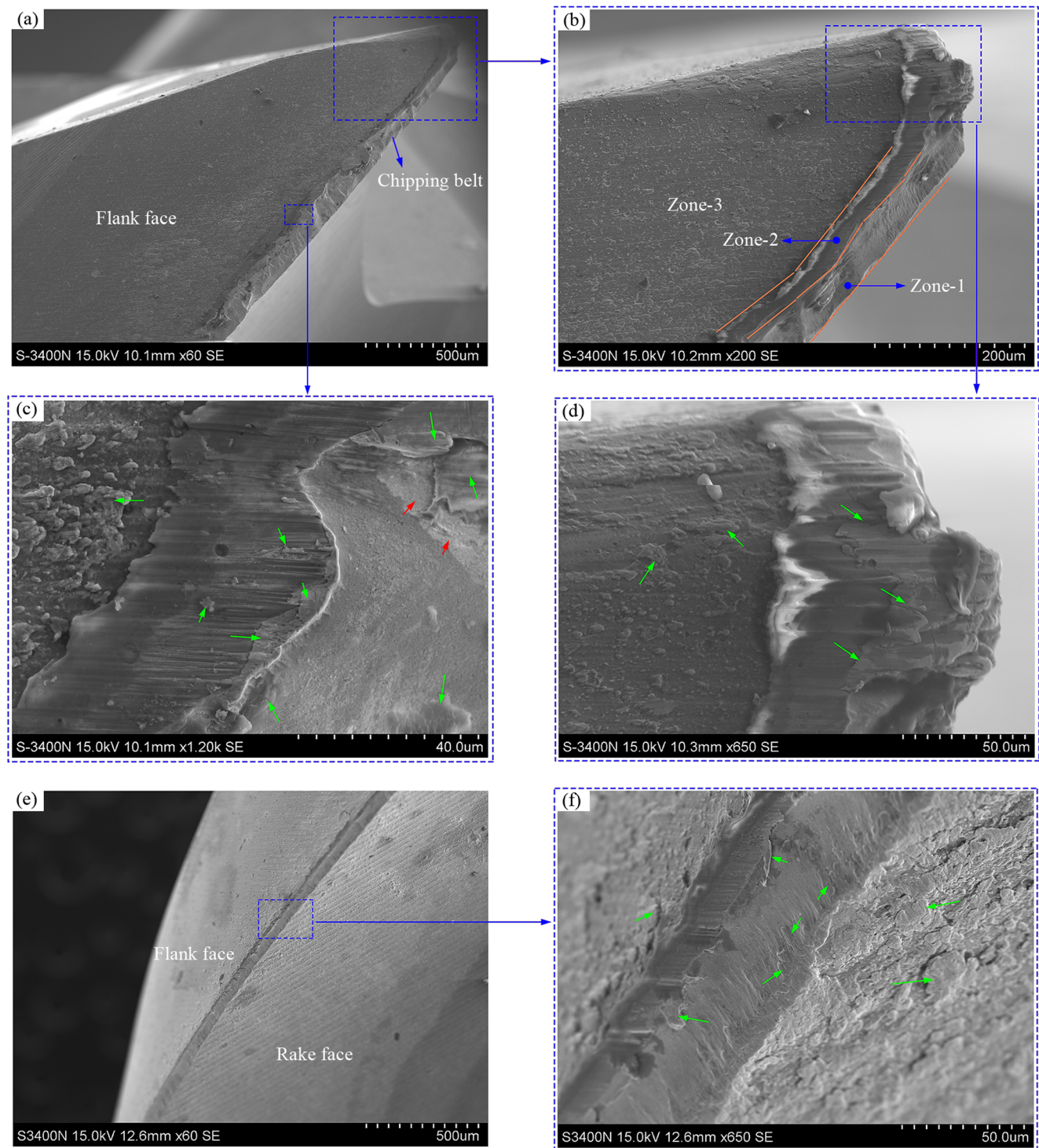


Fig. 10 SEM images of worn tool of compressed air cooling method with a cutting distance of 110 m. **a** Flank face of the tool. **b** Flank face near the tip. **c** Partial enlarged view. **d** Partial enlarged view. **e** Rake and flank faces and the chipping belt. **f** Partial enlarged view

removal effect and lubrication ability of OoW than dry cutting and compressed air cooling, tool wear, chipping, and adhesion are controlled to some extent, which delayed the evolution of the milling force.

In Fig. 12b, the x -direction milling force of OoW did not change significantly during the stable tool wear stage

(40–120 m), and exhibited a slow downward trend in the rapid tool wear stage (120–180 m). This may be related to the gradual peeling of the cutting-edge material, which requires further analysis, to be addressed later. In the late wearing stage of the tool in compressed air cooling and dry cutting, the x -direction milling force did not decrease

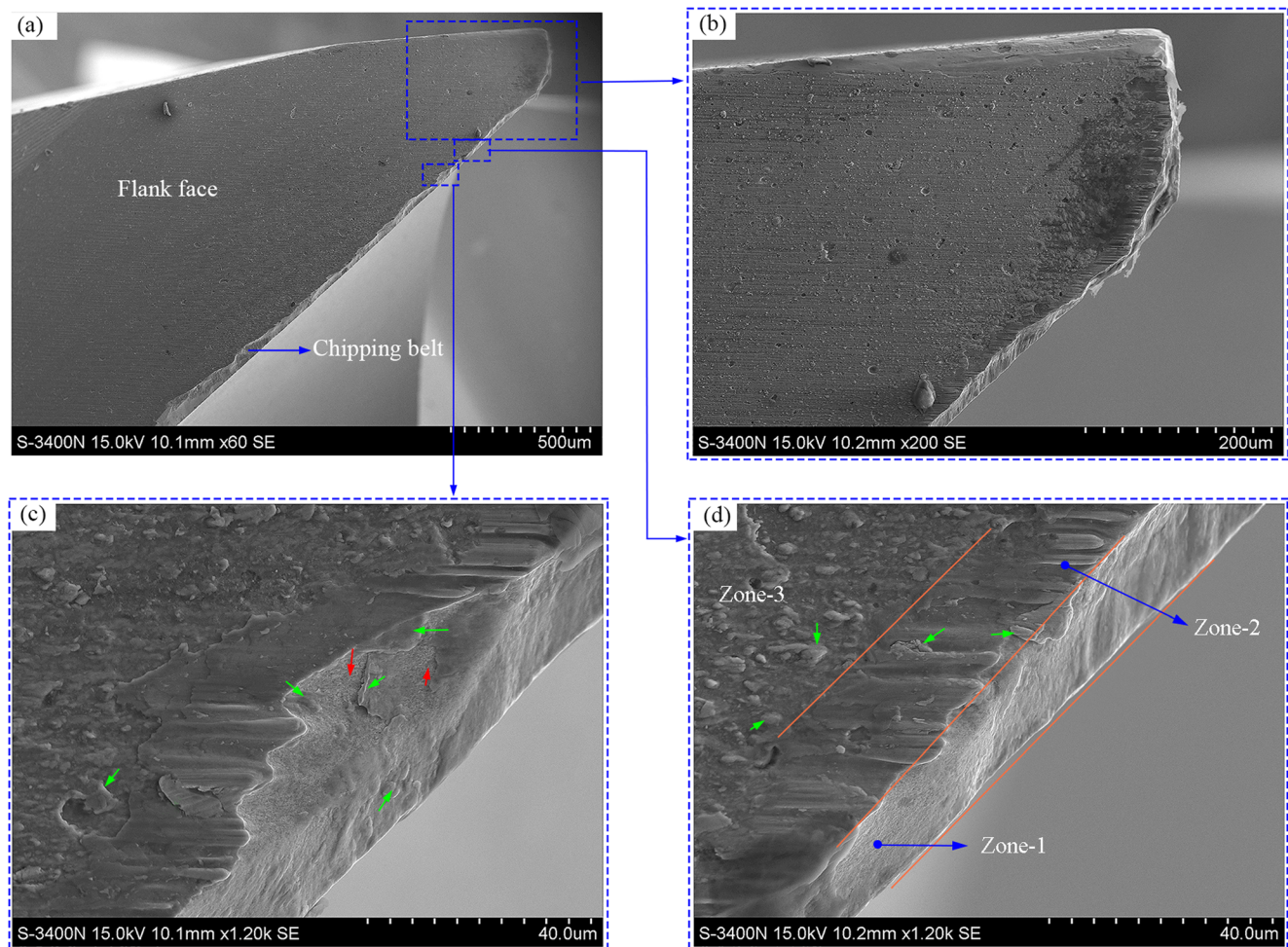


Fig. 11 SEM images of the tool of OoW method at a cutting distance of 180 m. **a** Flank face of the tool. **b** Flank face near the tip. **c** Partial enlarged view. **d** Partial enlarged view

but showed a significant upward trend, which may be related to the increasing material adhesion.

4 Discussion

4.1 Cooling and lubrication of compressed air cooling and OoW methods

4.1.1 Comparison of heat transfer coefficients of the three methods

When the heat generated from the cutting zone is removed by heat convection, the heat removal rate depends on the physical ability of the coolant. Fourier's law of conductive heat transfer indicates that the heat flux (q) is given by

$$q = k\Delta T = k(T_o - T_j) \quad (3)$$

In this formula, T_o is the object surface temperature, T_j is the coolant jet temperature, and k is the heat transfer coefficient. According to Eq. (3), when the temperature variation is constant, the heat removal capacity increases with increasing heat transfer coefficient.

The heat transfer of the compressed air cooling approach is much greater than that of the dry cutting method. The temperatures measured in [20, 21] for the dry cutting approach provide evidence. The compressed air cooling approach can reduce the cutting temperature by 15–25% compared with that of the dry cutting method with different cutting parameters [20, 21]. The OoW approach uses compressed gas with the same pressure and flow rate as the compressed air cooling method. For pure gas, the heat transfers of the two methods are comparable. However, the amounts of water and trace oil have to be considered in the OoW method. When water is mixed with compressed gas and becomes atomized to form a two-phase jet, a heat transfer coefficient of approximately 22 times that of the compressed gas approach can be obtained [22].

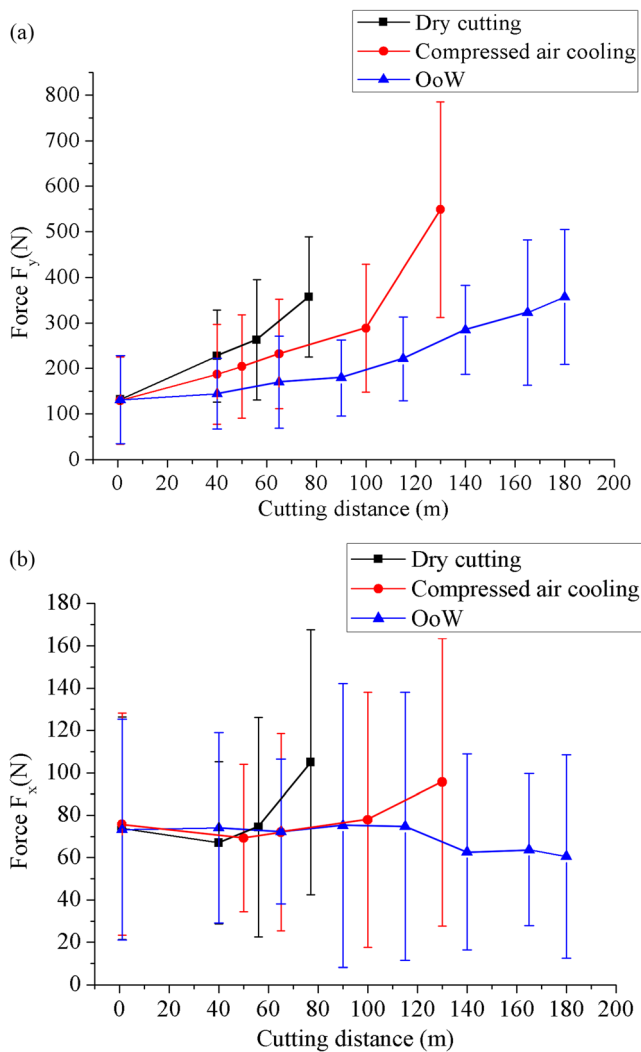


Fig. 12 Milling force at the cutting speed of 170 m/min. **a** y-direction. **b** x-direction

Therefore, the heat transfer coefficients of the OoW, compressed air cooling, and dry cutting methods decrease in this order, and that of the OoW method is significantly greater.

4.1.2 Cooling and lubricating of compressed air cooling method

In deep-cut high-speed milling of hardened steel, shearing and friction generate a large amount of cutting heat. Dry cutting has lower heat transfer and the cutting heat removed by air is also limited. Moreover, there is a gas barrier layer in high-speed milling, and the chips are difficult to discharge. These result in more heat accumulated on the tools. Thus, the temperature of the cutting edge of dry cutting is relatively higher with severe thermal wear such as adhesion. As shown in Figs. 6 and 9, at both cutting speeds (130 and 170 m/min), the flank face at zones 1–3 generates significant bonds.

To cool and lubricate the cutting tools and lengthen their life in compressed air cooling and OoW, the following prerequisites should be met first: the gas velocity is higher than the peripheral velocity of the rotating tool, and the gas is able to penetrate the tool/chip/workpiece interfaces. According to López de Lacalle et al. [18] and An et al. [22], the injection speed of the compressed gas can reach 120–300 m/s, which is much faster than the cutting speed of 3 m/s. According to Klocke et al. [23], whether the jet can intervene in the cutting zone is closely related to the jet pressure. Klocke et al. [23] presented the following formula:

$$\frac{F_{\text{jet}}}{A_{\text{jet}}} = 2 \times (p - p_{\text{ambient}}) \quad (4)$$

Equation (4) reveals that the mechanical pressure of the jet depends exclusively on the jet supply pressure. High-pressure gas is applied both in air cooling and OoW, whose mechanical pressure is sufficient to break through the gas barrier layer created by the tool's rotation.

Owing to the high-speed and high-pressure features, the air jet of the compressed air cooling approach can enter the cutting interfaces between the tool and chips and the tool and workpiece for effective cooling and lubrication. A significant amount of heat is removed by the compressed gas, which decreases the cutting temperature effectively. The direct benefit of the low temperature in the cutting zone is the reduction of diffusion and adhesion phenomena, which maintains the strength and creep resistance of the cutting edge and, thus, decreases the tool wear and breakage [20]. Compared with those of the dry cutting method, the tool lives of the compressed air cooling approach at 130 and 170 m/min cutting speeds are 45 and 48% higher, respectively; this is the direct result of the effective heat removal and temperature reduction in the cutting zone. However, at higher cutting speed (170 m/min), there is still evident adhesion at the later stage of tool wear (Fig. 10), indicating certain limitations of the heat removal capability in compressed air cooling.

4.1.3 Cooling and lubricating of the OoW method

In the OoW approach, oil, water, and gas are mixed to form atomized jets. The high-pressure gas carrying atomized microdroplets can break through the gas barrier layer into the cutting contact zone. The water is mainly responsible for cooling, which increases the heat transfer coefficient of the OoW method significantly compared with that of the compressed air cooling approach. The oil is mainly responsible for lubrication, thereby reducing the cutting heat generation. Owing to the good cooperation between the oil, water, and gas, the OoW method exhibits an excellent thermal removal ability, and the cutting temperature can be effectively controlled at a lower level. The high-temperature wear mode of

the OoW approach (e.g., adhesion) is significantly less severe than that of the compressed air cooling approach. Based on the good heat removal and lubrication abilities, the OoW method delays the tool wear process and extends the tool life considerably. At 130 and 170 m/min cutting speeds, the tool lives of OoW are, respectively, 44 and 86% longer than those of the compressed air cooling method. In addition, the tool life of the OoW method is not affected by the cutting speed. At a high cutting speed (170 m/min), the tool life of OoW is slightly higher than the tool life at a low cutting speed (130 m/min) (Figs. 5 and 8). However, the tool life of both dry cutting and air cooling approaches is easily affected by the high heat caused by the high cutting speed (Figs. 5 and 8). Evidently, the OoW method exhibits a more excellent cooling and lubricating performance and is suitable for cutting at high cutting speeds.

Water and trace oils are indispensable in the OoW method. If the oil mist (MQL) and water mist are sprayed separately, the tool wear proceeds significantly faster than in the OoW method, as shown in Fig. 13. The OoW approach is evidently

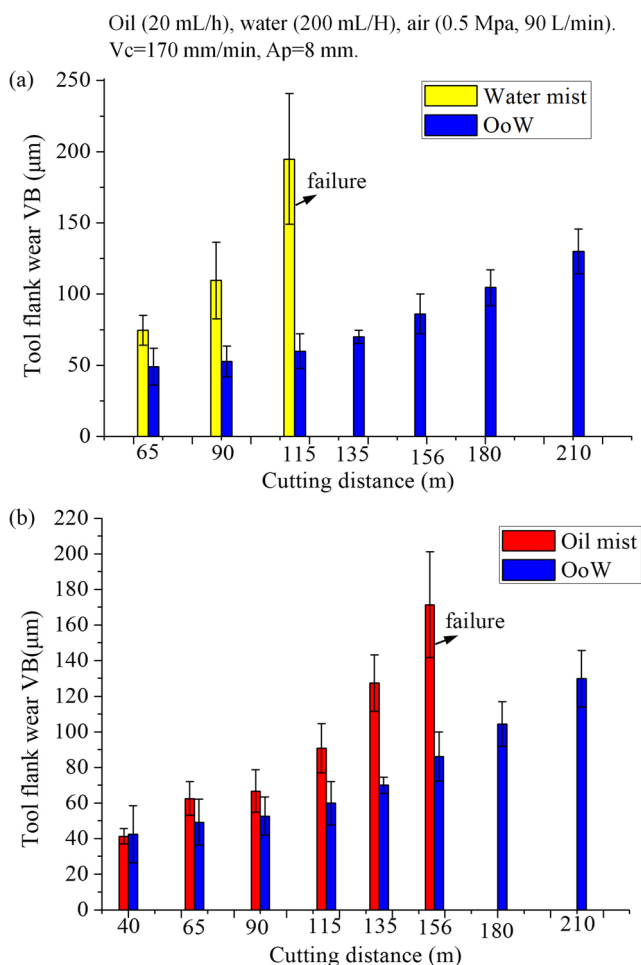


Fig. 13 Comparison of tool wear under three conditions. **a** Water mist and OoW. **b** Oil mist and OoW

superior to the separate use of water and oil mists, which should be related to its special cooling/lubrication mechanism.

The cooling and lubrication mechanisms of the OoW method can be explained with Fig. 14. The OoW approach results in a high number of droplets. The body of each droplet is composed of water, and the outer surface is covered by an oil film. When these droplets collide with the hot tool face, they are flattened owing to inertia, and their top membrane breaks owing to the high tension and increasing temperature. Subsequently, the droplets spill around and form a double-layer film structure (Fig. 14b). When the oil film is applied to the blade surface, the water film resides over the oil film. Moreover, the oil film absorbs the heat of the tool, and the water film absorbs the heat of the oil film. Because the flash point of oil (300 °C) is higher than the boiling point of water (100 °C), the water film evaporates after absorbing the heat. This decreases the temperature of the tool and oil film and prevents a high-temperature failure of the oil film. Furthermore, the oil film on the blade surface is applied to the cutting zone by capillary tubes to provide good lubrication. If the water flow rate is high, the OoW formation does not occur; instead, a water-on-oil formation is created (Fig. 14c). The water-on-oil droplets form a two-layer film on the blade surface, and the oil film is stretched over the water film. When boiled by the high temperature of the blade surface, the water film generates bubbles that can break through the oil film. This may cause the oil splash and decrease the lubrication effect. This explains why the tool treated with the water-on-oil approach in Fig. 4 wears faster than the tool treated with the OoW approach. When the oil and water mists are sprayed separately, the droplets hit the blade surface and form a single-layer film. A single-layer oil film is prone to a high-temperature failure, and a single-layer water film exhibits a very poor lubrication effect. Therefore, the tool lives of the oil mist (MQL) and water mist methods are shorter than that of the OoW approach (Fig. 13).

4.2 Evolution of tool wear and breakage in dry cutting, compressed air cooling, and OoW cutting methods

The milling process is a typical interrupted cutting method. The tool is subjected to high cyclic thermomechanical impacts and cyclic stresses in the high-speed milling process, resulting in wear and breakage (e.g., abrasive wear, adhesive wear, diffusion wear, chipping, and tip breakage) [16, 24, 25]. These wear and breakage forms may occur in the high-speed deep milling by different cooling and lubricating methods in this study. In both the steady and rapid wear stages of the three processing methods, the tools have an evident chipping belt, which occupies most of the flank wear band. Understanding the formation and development of chipping belts is crucial for understanding the tool wear and breakage mechanism.

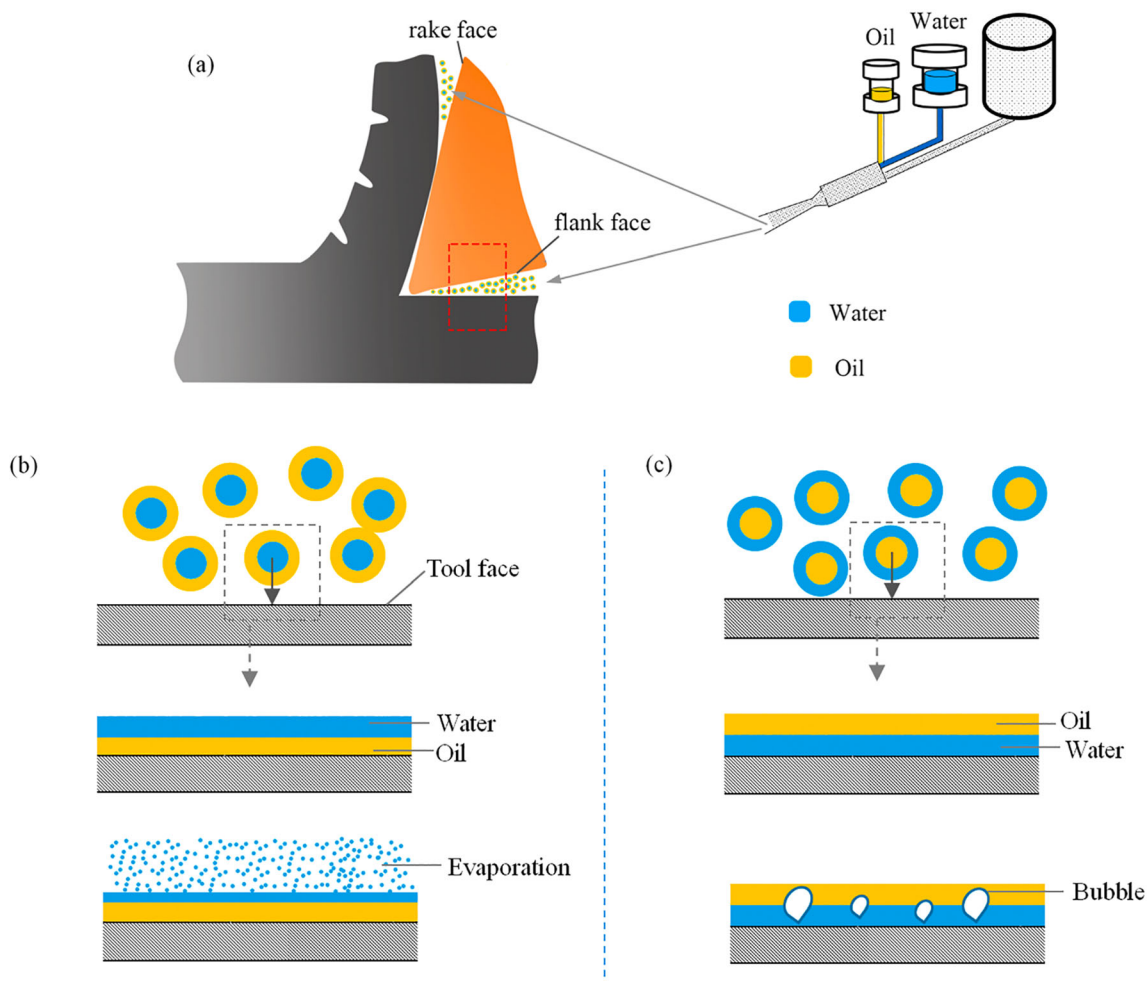


Fig. 14 Analysis of cooling and lubrication performances. **a** Spraying atomized droplets. **b** OoW mode. **c** Water-on-oil mode

4.2.1 Main wear and breakage forms of dry cutting, compressed air cooling, and OoW methods

Abrasion is one of the main tool wear mechanisms and can promote the tool wear and chipping development significantly [26]. All three cooling and lubrication methods exhibit significant abrasion on the tool flank faces and no evident abrasion on the rake faces. On machined tools at the cutting speeds of 130 and 170 m/min (Figs. 6, 9, 10, and 11), ridges parallel to the cutting direction can be clearly observed in zone 2 of the flank face. This is a typical indication of abrasion wear. From the EDS analysis, it can be determined that the grooves and ridges of zone 2 are coating elements. There are no significant grooves or ridges in the chipping belt of the flank zone 1. From these phenomena, the role of abrasion wear in the development of the wear belt can be concluded to consist mainly of the following two aspects. First, coating wear is a prelude to the formation of the chipping belt, whereas abrasion wear is the main form of wear. Second, as the surface coating is gradually worn and the tool substrate is gradually exposed, the chipping belt is expanded accordingly. For the bare chipping

belt, abrasion may still play a role in its wear, but other wear forms will gradually become dominant.

Adhesion is another main tool wear type. The dry cutting and compressed air cooling methods result in significant adhesion. Adhesion of the workpiece material can be observed on the rake and flank face. As shown in Figs. 6, 9, and 10, in dry cutting and compressed air cooling, certain adhered materials appeared on the rake face and more evident adhered materials on the flank face. These adhered materials are difficult to remove with ultrasonic oscillation, reflecting that strong bonds have been formed between the sticking substances and the tool. When the adhering materials are hit and squashed by the tool during the re-entry into the workpiece, tool wear and chipping become aggravated [27]. In the dry cutting and compressed air cooling procedures, most adhesion material resides mainly on the flank face than on the rake face (Figs. 9 and 10). Therefore, there is a strong adhesion interaction between the tool flank face and workpiece, which promotes the development of the chipping belt of the flank face. High cutting temperature provides a good environment for the formation of adhesion. The dry cutting method results in a

higher cutting temperature, and more adhesives are found in the chipping belt and its surrounding area, which eventually leads to rapid tool failure. The limited heat transfer in the compressed air cooling process makes it difficult to remove the heat in the later tool wear stage effectively, thereby causing evident adhesion in the chipping belt. In addition, in the dry cutting and air cooling processes, the adhesion at the high cutting speed (170 m/min) is more serious than that at the low cutting speed (130 m/min). Hence, the high cutting temperature is an important cause of adhesion.

Attrition is another wear type that is closely related to adhesion. Both play important roles in the formation and development of a chipping belt in the dry cutting and compressed air cooling processes. Owing to the intermittent attachment and detachment of the workpiece material, small fragments of the tool material are plucked and removed by the irregular attrition [28], thereby resulting in unevenly worn surfaces. The attrition phenomenon can be seen on the flank face of the tools treated with the dry cutting and compressed air cooling methods. As shown in Figs. 9 and 10, rough attrition regions (indicated by red arrows) occur in the chipping areas and surrounding areas of the flank faces. Attrition is severe at high cutting speeds and slight at low cutting speeds. Therefore, high cutting temperatures are an important reason for attrition.

Compared with the dry cutting and compressed air cooling methods, the OoW approach exhibits a better heat removal performance, which enables an effective control of the cutting zone temperature. Whether at a low cutting speed (130 m/min) or high cutting speed (170 m/min), the adhesion/attrition is much lower than those of the other two methods. Therefore, compared with the other two methods, the effect of adhesion/attrition in the development of the chipping belt in OoW is weakened to a certain extent. However, as the cutting speed increases, the adhesion/attrition may still play a role in the development of the chipping belt in OoW.

Tool wear is accompanied by tool breakage. During the formation and gradual expansion, the chipping/flaking belt of the flank is also accompanied by spalling of the tool material near the cutting edge. The material loss of the spiral end mill is difficult to quantify by common methods. In this study, through 3D tool scanning, a 3D model of the broken tool is established, as shown in Fig. 15. Figure 15a slices the 3D scanned tool through a plane perpendicular to the tool axis to obtain a cross-sectional outline with four tips. For each tip, extensions of the rake face curve and the flank curve are made and intersect at a point. Three parameters can be defined based on Fig. 15a: the spalling width S , chipping depth in the flank face D_f , and chipping depth in the rake face D_r . The main tip shapes of dry cutting, compressed air cooling, and OoW are shown in Fig. 15b. In general, D_f is greater than D_r , indicating that flank wear is the main cause of tool wear and breakage. In addition to the same form as is in dry cutting

and compressed air cooling, OoW has another major form, which may be related to OoW's lower cutting temperatures, lighter adhesion, and stronger mechanical impact. The most severe worn cutting edges of the failed tools in three methods were quantitatively analyzed and the results are shown in Fig. 15c and d. Dry cutting, the worst cutting environment, produces the largest S value, and OoW with its good cooling and lubrication produces the smallest. The spalling width of tool materials is very large compared with the flank wear value VB . The material peeling width is over 30% of the flank wear band value VB . Evidently, during the development of the chipping/flaking belt, the tool material is gradually lost, which has an important impact on tool failure. In addition, tool breakage has a significant influence on the milling force. In Figs. 7b and 12b, the x -direction milling force of the OoW tool decreases gradually. This is probably the result of the tool material loss. In addition, because the tool material is gradually lost, the degree of the cutting-edge passivation may gradually increase, resulting in a gradual increase in the y -direction milling force (Figs. 7a and 12a).

4.2.2 Generation and development of chipping belt

In dry cutting, compressed air cooling, and OoW, the main part of the tool flank wear land is the chipping belt. Therefore, the formation and development of the chipping belt is the key to the wear and breakage process of the spiral end mill. The formation and development of chipping is related to four types of factors: (1) mechanical cracks [14], (2) thermal stress and fatigue [27, 29, 30], (3) mechanical behavior of WC–Co composites [31], and (4) adhesion/attrition and abrasion (see Section 4.2.1). There are some differences in the factors that form the chipping belt in the three cooling/lubrication methods. Of the three methods, dry cutting and OoW represent two extremes. Dry cutting lacks cooling and lubrication, leading to a high cutting-edge temperature and a small gradient of the cutting-edge temperature in interrupted cutting. OoW has very good cooling and lubrication, and thus, its temperature change gradient of the cutting edge in interrupted cutting is larger. The characteristics of the air cooling mode are between those of dry cutting and OoW. The following analysis focuses on dry cutting and OoW.

In the dry deep-cut high-speed milling mode, the temperature gradient of the cutting edge at each turn of cutting in and out is small. The chipping belt on the flank face exhibits good continuity (Fig. 6a and Fig. 9a). In the early stages of tool wear, abrasion is the primary form. In the stable stage of tool wear, the bandwidth of the continuous chipping belt gradually expands, and the adhesion/attrition gradually replaces abrasion as the main wear factor. In the fast wear stage, owing to the high cutting temperature, the adhesion/attrition is particularly serious, and the deteriorating diffusion and oxidative wear also reduce the strength of the cutting edge. The cutting

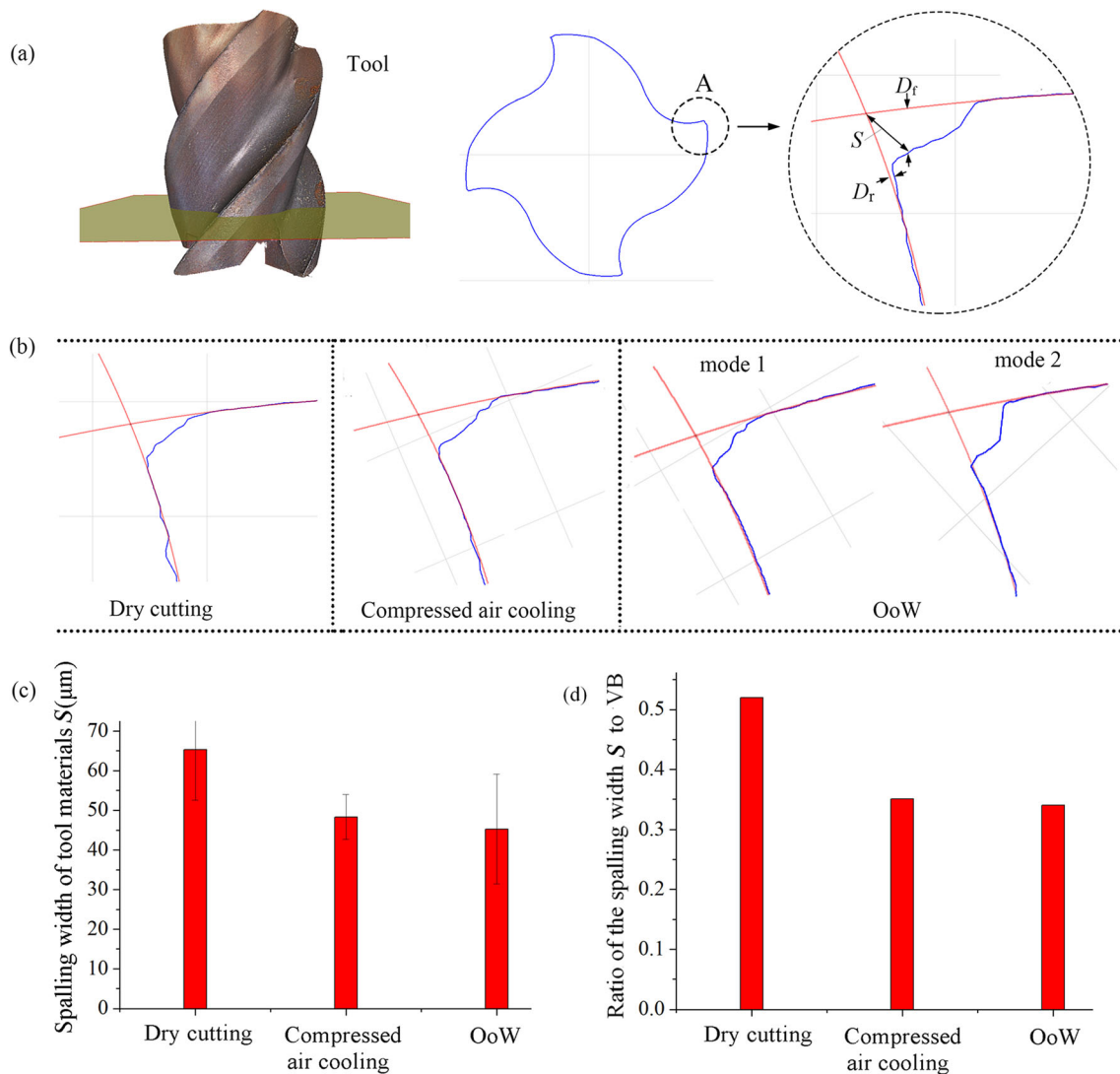


Fig. 15 Quantitative analysis of tools at 170 m/min cutting speed. (a) 3D scanning tool and contour curve of one cross-section; (b) Main shapes of tips of dry cutting, compressed air cooling, and OoW methods; (c)

Comparison of spalling width of tool materials; (d) Ratio of spalling width S to flank wear VB

force is also relatively large at this stage (see Fig. 7 and Fig. 12), and the tool is subjected to larger mechanical shocks. Owing to the lack of cooling and lubrication during the entire wear process, the chipping belt develops very quickly and is accompanied by a certain amount of material peeling, resulting in rapid tool failure.

Compared with dry cutting, there are two significant differences in the OoW cutting process. First, the cutting temperature is well controlled, and the effect of the adhesion/attrition in the development of the chipping belt is relatively reduced. Second, the generation and development of the chipping belt has always been in a discontinuous state (Fig. 6a and Fig. 11a). In the early tool wear stage of OoW cutting, discontinuous microchipping gradually occurs, whose main reasons can be found through exclusion analysis. First, the wear of the tool coating and substrate is relatively light in the initial stage

of tool wear, and the effect of abrasion and adhesion/attrition is also relatively small. Therefore, abrasion and adhesion/attrition are not the main reasons for OoW's discontinuous microchipping. Second, in the initial stage of tool wear, the differences in cutting force among the three methods are small (see Fig. 7 and Fig. 12). Therefore, a mechanical shock may have a certain impact on the discontinuous microchipping in the OoW process; nevertheless, it is not the main reason. Third, the other two possible factors, thermal fatigue and mechanical behavior of the tool substrate in a certain temperature range, are difficult to exclude under existing experimental conditions. During each turn of the OoW's tool from cutting out to cutting into the workpiece, the cutting edges are subjected to OoW jet chilling, resulting in a large temperature gradient and thermal stress. Owing to the helix angle influence of end mill, different edge areas of the cutting edge gradually

cutting into the workpiece at each turn will further increase temperature differences and local thermal stresses in different edge areas. Cyclic thermal stress can cause thermal fatigue, thereby causing the cutting edge to be prone to discontinuous microchipping. In addition, cemented carbide tools exhibit certain brittleness in a temperature range (close to and below 500 °C) [31]. In this case, discontinuous microchipping can be easily induced by a mechanical load. Thus, the thermal fatigue and mechanical behavior of the tool substrate in a certain temperature range are probably the most important reasons for the discontinuous microchipping of OoW tools in the early tool wear stage. As the wear process enters the stable tool wear and later stages, the thermal fatigue and mechanical behavior of the tool substrate in a certain temperature range remain two of the important reasons for the OoW chipping expansion. In addition to the comparison experiments of the OoW and dry cutting methods (Figs. 6, 9, and 11), the comparative experiments at different OoW water flow rates (Fig. 4) provide evidence for the previously presented correlation analysis of the chipping, thermal stress, and tool material properties. Furthermore, no evident thermal cracks and only mechanical impact cracks were found in the OoW failure tool (Fig. 4). When the cemented carbide tool has ultrafine WC grains (Fig. 1), a high Co content, and trace amounts of Ti, Cr, and Nd carbides (TiC, CrC, and NdC), its breaking strength is considerably enhanced. Although the thermal stress generated in the OoW process may be high, it does not exceed the breaking strength of the existing tools and cannot directly induce coarse thermal cracks. However, the thermal stress and a mechanical shock can form complex internal stresses, which increase the possibility of local material peeling.

The impact load promotes the development of a chipping belt on the OoW tool after discontinuous chipping has formed. When a portion of the discontinuous chipping area is located at the cutting edge, the other portions of the edge protrude correspondingly and must bear the entire milling force. Therefore, the protruding portion is subjected to a significantly increased mechanical stress. Yang et al. [32] studied the edge chipping mechanism of ceramic material milling. The edge chipping behavior of ceramics has similar mechanical characteristics. Under a high mechanical stress, the material protruding from the cutting edge peels off and reaches a temporary balance. Subsequently, the local thermal stresses, thermal fatigue, and mechanical stress again lead to the formation of new chippings. This “protrude–peel off–balance–protrude” cycle is accompanied by the development of a chipping belt until the OoW tool failure occurs.

The workpiece surface roughness provides supporting evidence for the previously presented analysis (Fig. 16). The surface roughness refers to the unevenness of tiny peaks and valleys on the machined surface. It is closely related to the contact friction between the tool and workpiece. As a typical characterization parameter for the surface roughness, R_a is the

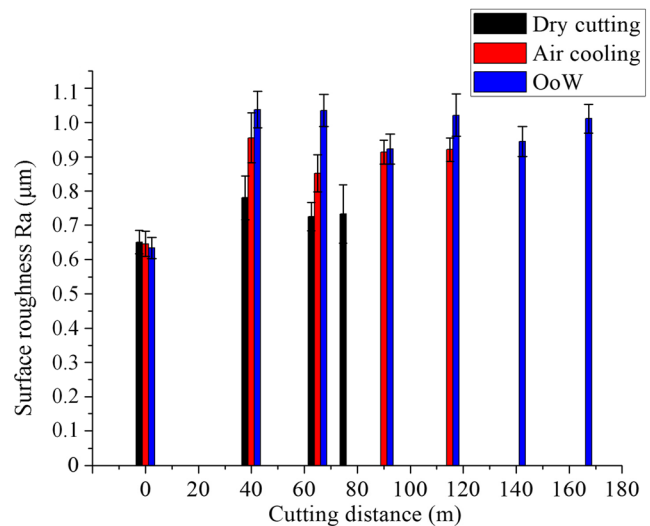


Fig. 16 Comparison of surface roughness of dry cutting, compressed air cooling, and OoW methods at 170 m/min cutting speed

arithmetic average of the distances from each point of the cross-section contour to the datum line within the sampling length. In this study, the surface roughness R_a was measured at the half axial depth of cut. The surface roughness values R_a of the three methods are similar at a cutting length of 1 m. However, when the cutting edges form discontinuous chipping, the workpiece surface roughness can be increased. In the dry cutting process, the change in the temperature gradient is minimal, the continuity of the chipping belt is the best, and the surface roughness is the smallest. Moreover, the OoW method results in the highest surface roughness at a cutting length over 40 m. At cutting lengths of 90 and 140 m, the two surface roughness values of the OoW method decrease suddenly, which corresponds to a brief equilibrium period when the protruding material peels off the edge.

5 Conclusions

The feasibility of the OoW method in the high-speed deep milling process of hardened steel with a coated carbide tool was investigated in this study. The conclusions are as follows:

1. The spraying angle and flow rate of water are important parameters that affect the tool life in OoW milling.
2. OoW has significantly better heat removal and lubrication than dry cutting and air cooling. Compared with dry cutting and air cooling, OoW considerably lengthens tool life by 169 and 86% at the cutting speed of 170 m/min and by 112 and 44% at 130 m/min.
3. Water and trace oils are indispensable for the OoW method. When the OoW droplets collide with the cutting interface, a two-layer film is formed. The evaporation of the water film removes much heat and prevents the high-

temperature failure of the oil film. When the oil and water mists are sprayed separately, the droplets hit the blade surface and form a single-layer film structure. The single-layer oil film is prone to a high-temperature failure, and the single-layer water film exhibits a poor lubrication performance. Therefore, the tool lives of oil mist (MQL) or water mist-treated samples are evidently shorter than those of tools treated with OoW.

4. The chipping belt occupies most of the flank wear land. Its formation and development are the key to the wear and failure of the cemented carbide spiral end mill. The development of tool wear and the chipping belt is also accompanied by a certain amount of material peeling loss.
5. The chipping belts of dry cutting and air cooling are both in the continuous stage. Adhesion/attrition and abrasion wear are the primary wear mechanisms. In OoW cutting, the chipping belt is in a discontinuous state, on which the effect of the adhesion/attrition is weaker compared with that of the other two methods. The thermal fatigue and mechanical behavior of the tool substrate in a certain temperature range are the main reasons for the discontinuous chipping belt in the OoW procedure. The increase in the workpiece surface roughness confirms the discontinuity of the chipping belt.

Funding information The work reported herein was supported by the “National Science and Technology Major Project (2018YFB2002200),” “Science and Technology Program of Guangdong Province (2017A010102011),” “Natural Science Foundation Project of Guangdong Province (2018A0303130107),” and “Education Committee Project of Guangdong Province (2015KTSCX028).”

Compliance with ethical standards

Conflict of interest The authors declare that they have no conflict of interest.

References

1. Wu SX, Ma W, Li B, Wang CH (2016) Trochoidal machining for the high-speed milling of pockets. *J Mater Process Technol* 233:29–43
2. Wu SX, Li ZY, Wang CY, Li SY, Ma W (2018) Tool wear of corner continuous milling in deep machining of hardened steel pocket. *Int J Adv Manuf Technol* 97(1–4):1–19
3. Schoop J, Sales WF, Jawahir IS (2017) High speed cryogenic finish machining of Ti-6Al4V with polycrystalline diamond tools. *J Mater Process Technol* 250:1–8
4. Sun SJ, Brandt M, Palanisamy S, Dargusch MS (2015) Effect of cryogenic compressed air on the evolution of cutting force and tool wear during machining of Ti-6Al-4V alloy. *J Mater Process Technol* 221:243–254
5. Stephenson DA, Skerlos SJ, King AS, Supekar SD (2014) Rough turning Inconel 750 with supercritical CO₂-based minimum quantity lubrication. *J Mater Process Technol* 214(3):673–680
6. Liao YS, Lin HM, Chen YC (2007) Feasibility study of the minimum quantity lubrication in high-speed end milling of NAK80 hardened steel by coated carbide tool. *Int J Mach Tools Manuf* 47(11):1667–1676
7. Khettabi R, Nouioua M, Djebara A, Songmene V (2017) Effect of MQL and dry processes on the particle emission and part quality during milling of aluminum alloys. *Int J Adv Manuf Technol* 92(5–8):2593–2598
8. Ganguli S, Kapoor SG (2016) Improving the performance of milling of titanium alloys using the atomization-based cutting fluid application system. *J Manuf Process* 23:29–36
9. Yoshimura H, Itoigawa F, Nakamura T, Niwa K (2005) Development of nozzle system for oil-on-water droplet metalworking fluid and its application to practical production line. *JSME Int J Ser C* 48(4):723–729
10. Itoigawa F, Childs THC, Nakamura T, Belluco W (2006) Effects and mechanisms in minimal quantity lubrication machining of an aluminum alloy. *Wear* 260(3):339–344
11. Wang CY, Lin HS, Wang X, Zheng LJ, Xiong WQ (2017) Effect of different oil-on-water cooling conditions on tool wear in turning of compacted graphite cast iron. *J Clean Prod* 148:477–489
12. Junior AB, Diniz AE, Filho TF (2009) Tool wear and tool life in end milling of 15–5 PH stainless steel under different cooling and lubrication conditions. *Int J Adv Manuf Technol* 43(7–8):756
13. Nouari M, Ginting A (2006) Wear characteristics and performance of multi-layer CVD-coated alloyed carbide tool in dry end milling of titanium alloy. *Surf Coat Technol* 200(18–19):5663–5676
14. Liew WYH, Ding X (2008) Wear progression of carbide tool in low-speed end milling of stainless steel. *Wear* 265(1–2):155–166
15. Dolinšek S, Šuštaršič B, Kopač J (2001) Wear mechanisms of cutting tools in high-speed cutting processes. *Wear* 250(1–12):349–356
16. Wang CY, Xie YX, Qin Z, Lin HS, Yuan YH, Wang QM (2015) Wear and breakage of TiAlN- and TiSiN-coated carbide tools during high-speed milling of hardened steel. *Wear* 336–337:29–42
17. Iqbal A, Ning H, Khan I, Liang L, Dar NU (2008) Modeling the effects of cutting parameters in MQL-employed finish hard-milling process using D-optimal method. *J Mater Process Technol* 199(1–3):379–390
18. López de Lacalle LN, Angulo C, Lamikiz A, Sánchez JA (2006) Experimental and numerical investigation of the effect of spray cutting fluids in high speed milling. *J Mater Process Technol* 172(1):11–15
19. Vieira JM, Machado AR, Ezugwu EO (2001) Performance of cutting fluids during face milling of steels. *J Mater Process Technol* 116(2–3):244–251
20. Sun S, Brandt M, Dargusch MS (2010) Machining Ti-6Al-4V alloy with cryogenic compressed air cooling. *Int J Mach Tools Manuf* 50(11):933–942
21. Stanford M, Lister PM, Morgan C, Kibble KA (2009) Investigation into the use of gaseous and liquid nitrogen as a cutting fluid when turning BS 970-80A15 (En32b) plain carbon steel using WC-Co uncoated tooling. *J Mater Process Technol* 209(2):961–972
22. An QL, Fu YC, Xu JH (2011) Experimental study on turning of TC9 titanium alloy with cold water mist jet cooling. *Int J Mach Tools Manuf* 51(6):549–555
23. Klocke F, Sangermann H, Krämer A, Lung D (2011) Influence of a high-pressure lubricoolant supply on thermo-mechanical tool load and tool wear behaviour in the turning of aerospace materials. *Proc Inst Mech Eng B J Eng Manuf* 225(1):52–61
24. Koshy P, Dewes RC, Aspinwall DK (2002) High speed end milling of hardened AISI D2 tool steel (~58 HRC). *J Mater Process Technol* 127(2):266–273
25. Deng J, Liu J, Zhao J, Song WL (2008) Wear mechanisms of PVD ZrN coated tools in machining. *Int J Refract Met Hard Mater* 26(3):164–172
26. Shaikh V, Boubekri N, Scharf TW (2014) Analyzing the effectiveness of microlubrication using a vegetable oil-based metal working

- fluid during end milling AISI 1018 steel. *Int J Manuf Eng* 2014:1–13
27. Jawaid A, Sharif S, Koksai S (2000) Evaluation of wear mechanisms of coated carbide tools when face milling titanium alloy. *J Mater Process Technol* 99(1–3):266–274
 28. Haron CHC, Ginting A, Arshad H (2007) Performance of alloyed uncoated and CVD-coated carbide tools in dry milling of titanium alloy Ti-6242S. *J Mater Process Technol* 185(1–3):77–82
 29. Wang B, Yin W, Wang M, Zheng Y, Li X, Ma Z (2017) Edge chipping mechanism and failure time prediction on carbide cemented tool during drilling of CFRP/Ti stack. *Int J Adv Manuf Technol* 91(9–12):3015–3024
 30. Su Y, He N, Li L, Li XL (2006) An experimental investigation of effects of cooling/lubrication conditions on tool wear in high-speed end milling of Ti-6Al-4V. *Wear* 261(7–8):760–766
 31. Mari D, Gonseth DR (1993) A new look at carbide tool life. *Wear* 165(1):9–17
 32. Yang B, Shen X, Lei S (2009) Mechanisms of edge chipping in laser-assisted milling of silicon nitride ceramics. *Int J Mach Tools Manuf* 49(3–4):344–350

Publisher's note Springer Nature remains neutral with regard to jurisdictional claims in published maps and institutional affiliations.